A&A 450, 159–166 (2006)
DOI: 10.1051/0004-6361:20054112

Astronomy & Astrophysics

Chemical abundances in seven galactic planetary nebulae⋆

A. C. Krabbe and M. V. F. Copetti

Laboratório de Análise Numérica e Astrofísica, Departamento de Matemática, Universidade Federal de Santa Maria, 97119-900 Santa Maria, RS, Brazil
e-mail: angela@lana.ccne.ufsm.br

Received 27 August 2005 /Accepted 1 December 2005

ABSTRACT

An observational study of chemical abundances in the galactic planetary nebulae NGC 1535, NGC 2438, NGC 2440, NGC 3132, NGC 3242, NGC 6302, and NGC 7009 based on long-slit spectra of high signal-to-noise ratio in the 3100 to 6900 Å range is presented. We determined the N, O, Ne, S, and Cl abundances from collisionally excited lines and the He and O^{++} abundances from recombination lines. The O^{++}/H^+ estimates derived from recombination lines are about a factor of four and two higher than those derived from forbidden lines for NGC 7009 and NGC 3242, respectively. Spatial profiles of O^{++}/H^+ abundance from O II permitted lines and from [O III] forbidden lines were obtained for the planetary nebula NGC 7009. The differences between O^{++}/H^+ derived from recombination and from forbidden lines present smooth variations along the nebular surface of NGC 7009, with the differences decreasing from the center to the edges of the nebula. If these abundance differences are explained by the presence of electron temperature fluctuations, quantified by the parameter t^2, a value of about $t^2 = 0.09$ is required for NGC 3242 and NGC 7009.

Key words. ISM: planetary nebula: general – ISM: abundances

1. Introduction

Almost all the determinations of abundances of heavy elements in H II regions and planetary nebulae published up to now are based on the analysis of collisional excited emission lines, which depend exponentially on electron temperature. This fact makes necessary the use of precise determinations of electron temperature to obtain reliable estimates of ionic abundances. On the other hand, recently it has been possible to determine abundances of heavy elements from recombination lines, which have the advantage of being weakly dependent on the electron temperature and in principle can be reliable indicators of chemical abundances. However, these lines are very faint, about 10^3–10^4 times fainter than the strong forbidden lines, and thus are very difficult to detect and measure, mainly in objects with low surface brightness.

A common result reported in the literature is that the ionic abundances derived from recombination lines are systematically higher than those obtained from forbidden lines. These discrepancies can be very large, as for example, the factor of 10 found by Liu et al. (2000) in the CNO abundances for the planetary nebula NGC 6153. One potential explanation to these discrepancies would be the presence of temperature fluctuations inside of H II regions and planetary nebulae (Peimbert 1967). However, the observed values of electron temperature fluctuations have been lower than the ones necessary to reconcile the abundances derived from forbidden and permitted lines (Liu 1998; Rubin et al. 2002; Krabbe & Copetti 2002; Rubin et al. 2003; O'Dell et al. 2003; Krabbe & Copetti 2005). Other solution that was suggested by Liu et al. (2000) would be the presence inside the nebula of hydrogen deficient clumps with high density and rich in heavy elements. A support for this hypothesis could arise from spatial profiles of abundances of heavy metals determined from recombination lines and forbidden lines in nebulae. However, only for the planetary nebulae NGC 6153 (Liu et al. 2000) and NGC 6720 (Garnett & Dinerstein 2001) has such a study been done to date.

In our previous paper (Krabbe & Copetti 2005, hereafter Paper I), we presented a study on the spatial variation of electron density and temperature in a sample of galactic planetary nebulae. In the present paper we used the Paper I data to determine the ionic and total abundances of He, N, O, Ne, S, and Cl in the planetary nebulae NGC 1535, NGC 2438, NGC 2440, NGC 3132, NGC 3242, NGC 6302, and NGC 7009. A comparison between the spatial profiles of O^{++}/H^+ derived from forbidden and recombination lines in the planetary nebula NGC 7009 is also given. Section 2 describes the data utilized and the adopted procedures for determination of total and ionic abundances. The results and discussions are presented in Sect. 3 and the conclusions are given in Sect. 4.

2. Data analysis

The current paper is based on long slit spectrophotometry data in the range of 3100 to 6900 Å obtained on January,

⋆ Table 1 is only available in electronic form at http://www.edpsciences.org

July and December 2002 with the Boller & Chivens spectrograph attached to the 1.52 m telescope of the European Southern Observatory (ESO), Chile; and on September 1994 and May 2002 with the Cassegrain spectrograph of the 1.6 m telescope at the Laboratório Nacional de Astrofísica (LNA), Brazil. The slits used have entrances on the plane of sky of $2'' \times 250''$ for the observations at ESO and $2'' \times 320''$ for the observations at LNA. We used a Loral CCD of 2688×512 pixels at ESO and at LNA we used a SITe CCD of 1024×1024 pixels on May 2002 and an EEV CCD of 800×1024 pixels on September 1994. We used a grid of 1200 grooves mm^{-1} at LNA and at ESO we used a grid of 2400 grooves mm^{-1} during the January and July runs and a grid of 1200 grooves mm^{-1} during the December run. The spatial scale was $0.82'' \ pxl^{-1}$ for the Loral CCD, $0.90'' \ pxl^{-1}$ for the EEV CCD, and $1.0'' \ pxl^{-1}$ for the SITe CCD. The spectra obtained had a spectral resolution of 1.5 Å and 3.0 Å for the observations at ESO and 2.8 Å for the observations at LNA, measured as the full-width-at-half-maximum *FWHM* of the emission lines of the comparison lamps. In Paper I, we described the observations and the data reduction procedures with details.

Combining multiple exposures we have obtained a mean spectrum for each nebula after the integration of the light along the slit. The line intensities were obtained using Gaussian line profile fitting procedures. In the cases of line blending, we have employed multiple Gaussian profile fitting in order to deconvolve the lines and measure the line intensities of each individual line. These measurements were carried out with the *splot* routine of the *IRAF* package. All the line intensities of a given spectrum were normalized to Hβ. We estimated the error associated with the line flux intensities by $\sigma^2 = \sigma^2_{\rm cont} + \sigma^2_{\rm line}$, where $\sigma_{\rm cont}$ and $\sigma_{\rm line}$ are the continuum rms and the Poisson error of the line respectively. All the observed line intensities were corrected for the effect of the interstellar extinction. This correction was done by comparing the observed Hγ/Hβ and Hα/Hβ ratios with the theoretical ones by Hummer (1987) for an electron temperature of 10 000 K and a density of 100 cm^{-3}. The Galactic reddening function, $f(\lambda)$, of Savage & Mathis (1979) was used. Table 1 lists Galactic reddening function, $f(\lambda)$, the emission line intensities corrected by reddening $I(\lambda)$, and the logarithmic extinction coefficient c(Hβ) for each object. We have measured the Balmer jump by linearly fitting the observed continua on both sides of the discontinuity (see more details in Paper I).

2.1. Determination of electron density and temperature

Electron temperature estimates T_e(O III) and T_e(N II) were derived from the [O III](λ4959 + λ5007)/λ4363 and [N II](λ6548 + λ6583)/λ5755 intensity ratios and electron densities N_e(S II), N_e(Cl III), and N_e(Ar IV) from the [S II]λ6716/λ6731, [Cl III]λ5517/λ5537, and [Ar IV]λ4711/λ4740 intensity ratios, respectively. These electron temperatures and densities were obtained by numerically solving the equilibrium equations for an n-level atom using the *temden* routine of the *nebular* package of the *STSDAS/IRAF*, using the same atomic parameters and electron density and temperature adopted in Paper I. We have also calculated the electron temperature from the ratio of the nebular Balmer discontinuity to Hβ, $[F_\lambda(\lambda3646-) - F_\lambda(\lambda3646+)]/F(\mathrm{H}\beta)$ for NGC 1535, NGC 2440, NGC 3242, and NGC 7009. In Paper I we have discussed in detail the possible sources of uncertainty in the determination of electron temperature and density.

2.2. Determination of helium abundances

We derived the He^+/H^+ abundance from the emission lines λ4471, λ5876, and λ6678 and then averaged these abundances weighting according to the intensity of the line. The He^{++}/H^+ ratios were obtained from the He II λ4686 line. The recombination coefficients used were from Storey & Hummer (1995) for H and He II and from Benjamin et al. (1999) for He I, which includes the effects of collisional excitation from both 2^3 S and 2^1 metastable level. The elemental abundance of He was given by $He/H = He^+/H^+ + He^{++}/H^+$.

2.3. Determination of heavy abundances from collisional excited lines

We have derived ionic abundances of N, O, Ne, S and Cl from collisionally excited lines. These ionic abundances were derived by solving numerically the equilibrium equations for an n-level atom using the *abund* routine of the *nebular* package of the *STSDAS/IRAF*. The references used for the collision strengths C, transition probabilities A, and energy levels E are listed in Table 2.

The determination of ionic abundances derived from forbidden lines presents an exponential dependence on the assumed electron temperature. Therefore, appropriate temperatures must be adopted to calculate the abundance for a given ion. On the other hand, the dependence of ionic abundance estimates on the assumed electron density is insignificant. We have assumed the following scheme in the derivation of the ionic abundances: T_e(N II) and N_e(S II) were adopted for N^+, O^+, S^+ and S^{2+}, apart from the cases of NGC 1535 and NGC 3242, for which T_e(O III) was adopted instead, because T_e(N II) was not measured and NGC 1535, where N_e(Ar IV) was the only density estimate; T_e(O III) and a mean density obtained from N_e(Cl III) and N_e(Ar IV) were adopted for Cl^{++}, O^{++} and Ne^{++}; for Ne^{3+} and Ne^{4+} we used a mean density from N_e(Cl III) and N_e(Ar IV) and an electron temperature of T_e(O III) + 2270 K, which was indicated by Kingsburgh & Barlow (1994) based on the the results of photoionization models.

As discussed by Kingsburgh & Barlow (1994), the fractions of neutral heavy element are assumed to be the same as neutral hydrogen and therefore the final abundances relative to hydrogen are not altered. So, the abundances of neutral species were not derived. The total abundance for a given element was a sum of the ionic abundances. We used the ionization correction factors icf discussed by Kingsburgh & Barlow (1994) to correct for the unseen ions for a given element, except for Cl, which was not discussed by those authors. For Cl we assumed the

Table 2. References for the atomic data.

Ion	A	C	E
[N II]	[3]	[9]	[1, 2]
[O II]	[3]	[6, 7]	[1, 4, 5]
[O III]	[3]	[9]	[1, 8]
[Ne III]	[5, 10]	[11]	[1]
[Ne IV]	[13, 14]	[15]	[12]
[Ne V]	[5, 24]	[9]	[1, 10]
[S II]	[16, 17]	[18]	[1, 16]
[S III]	[5, 19, 20, 21]	[22]	[1]
[Cl III]	[10, 5]	[23]	[1]

References: [1] Bowen (1960); [2] Williams & Livio (1995); [3] Wiese et al. (1996); [4] Fawcett (1975); [5] Kaufman & Sugar (1986); [6] Pradhan (1976); [7] McLaughlin & Bell (1993); [8] Moore (1985); [9] Lennon & Burke (1994); [10] Mendoza (1983); [11] Butler & Zeippen (1994); [12] Moore (1971); [13] Becker et al. (1989); [14] Bhatia & Kastner (1988); [15] Giles (1981); [16] Verner et al. (1996); [17] Keenan et al. (1993); [18] Ramsbottom et al. (1996); [19] Mendoza & Zeippen (1982); [20] Heise et al. (1995); [21] LaJohn & Luke (1993); [22] Galavis et al. (1995); [23] Butler & Zeippen (1989); [24] Bhatia & Doschek (1993).

ionization correction factor adopted by Liu et al. (2000), based on the similarities of the ionization potentials of the Cl ion stages to those of the S ion stages. The errors in the ionic abundance were obtained by propagating the errors in electron temperature and line fluxes.

2.4. Determination of O^{++} abundance from recombination lines

The O^{++} abundance derived from observed recombination lines was obtained adopting the following equation:

$$\frac{O^{++}}{H^{+}} = \frac{I(O\,II,\lambda)}{I(H\beta)} \frac{\lambda(O\,II)}{\lambda(H\beta)} \frac{\alpha(H\beta)}{\alpha(O\,II,\lambda)}, \quad (1)$$

where $I(O\,II,\lambda)$ is the dereddened flux of a given emission line λ and α represents the recombination coefficient. The recombination coefficients depend only weakly on the adopted temperature and are essentially independent of the assumed density. For the calculation of O^{++} abundances we adopted the [O III] electron temperatures. The effective recombination coefficients used were from Storey (1994) for 3s–3p transitions and from Liu et al. (1995) for 3d–4f transitions, assuming case A for doublets and case B for quartets. The errors of O^{++} abundances were obtained by propagating the errors in the line fluxes.

We have derived O^{++} abundances for NGC 3242 and NGC 7009, the only planetary nebulae in our sample with good signal-to-noise ratios in O II emission lines. We also obtained a spatial profile of the O^{++} abundance for NGC 7009 from point-to-point measurements of the O II λ4661 line. Although this O II λ4661 line is blended with the [Fe III] + C IV λ4658 line, it could be deconvolved and measured accurately. In Fig. 1 a sample of the spectral region around 4661 Å for NGC 7009 is presented.

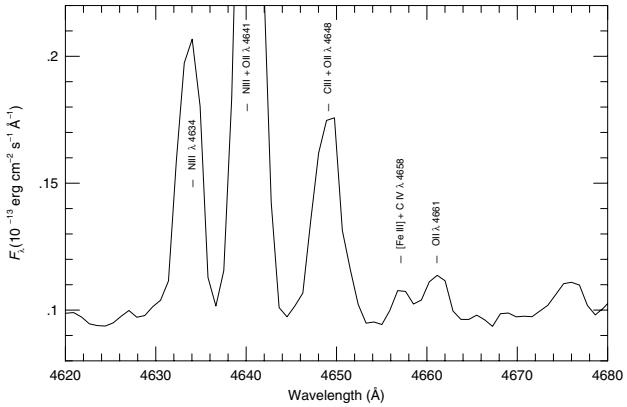

Fig. 1. A sample of the spectral region around 4661 Å for NGC 7009.

3. Results and discussions

3.1. Electron densities and temperatures

Table 3 presents the temperatures and densities estimated from the integrated spectrum for each planetary nebula in our sample. We have compared these estimates with those obtained from point-to-point measurements along the nebular surface published in Paper I. In general the estimates of electron temperatures and densities obtained from the integrated spectrum and from point-to-point measurements are consistent with each other within the error estimates, although some differences are found in some objects. These two methods provide mean values of electron temperatures and densities with different weights, so different mean temperatures and densities can be obtained from these methods. We can find differences in the estimates obtained with the two methods mainly in objects that presents systematic variations of electron temperature and density along the nebular surface. In particular, we have found large differences in the determinations of [S II] and [Cl III] electron densities for NGC 6302. The [S II] and [Cl III] densities of NGC 6302 obtained from the integrated spectrum are about 4500 cm^{-3} and 25 000 cm^{-3} lower than those derived from the point-to-point measurements. As this object shows an impressive spatial gradient of electron density, with the electron density peaking at the centre of the nebula and decreasing from the centre to the outer regions, we can expect higher densities derived from the point-to-point measurements (see Paper I).

3.2. Ionic and total abundances

Table 4 lists the He abundances derived from He I and He II recombination lines, the ionic and elemental abundances for heavy elements derived from forbidden lines, and the *icf* adopted. Table 5 presents a comparison between the elemental abundances derived in this paper and the ones previously published, expressed in units of log (X/H) + 12, for X = He, N, O, Ne, S and Cl. We verified that our elemental abundances are in good agreement with those obtained by other authors. Also, our estimations support the classification of NGC 2440, NGC 3132,

Table 3. Electron temperatures and densities.

Object	N_e (cm^{-3}) S II	N_e (cm^{-3}) Cl III	N_e (cm^{-3}) Ar IV	T_e (K) N II	T_e (K) O III	T_e (K) Bal
NGC 1535			1672 ± 101		11 765 ± 55	8990 ± 91
NGC 2438	143 ± 71		2206 ± 870	11 262 ± 360	11 192 ± 64	
NGC 2440	1807 ± 83	4898 ± 2097	2525 ± 122	11 670 ± 64	14 569 ± 22	12 693 ± 307
NGC 3132	637 ± 52	1289 ± 706	2265 ± 856	10 454 ± 78	9390 ± 112	
NGC 3242	1016 ± 255	2531 ± 1227	3665 ± 141		12 140 ± 31	9444 ± 41
NGC 6302	2183 ± 436	13 016 ± 4640	10 630 ± 137	14 381 ± 310	17 927 ± 61	
NGC 7009	3778 ± 227	5168 ± 384	5589 ± 128	10 128 ± 120	9969 ± 105	8690 ± 32

Table 4. Ionic and total abundances.

	NGC 1535	NGC 2438	NGC 2440	NGC 3132	NGC 3242	NGC 6302	NGC 7009
$10^2 \times He^+/H^+$	9.03 ± 0.36	8.63 ± 0.20	6.12 ± 0.92	11.99 ± 0.72	7.12 ± 0.13	8.64 ± 0.37	10.46 ± 0.67
$10^2 \times He^{++}/H^+$	1.45 ± 0.01	2.69 ± 0.01	6.59 ± 0.01	0.57 ± 0.02	3.47 ± 0.01	6.51 ± 0.05	1.42 ± 0.01
$10^2 \times He/H$	10.48 ± 0.36	11.32 ± 0.20	12.71 ± 0.92	12.56 ± 0.72	10.59 ± 0.13	15.15 ± 0.37	11.88 ± 0.67
$10^5 \times N^+/H^+$	0.011 ± 0.001	3.13 ± 0.07	7.44 ± 0.16	9.56 ± 0.24	0.019 ± 0.001	5.86 ± 0.44	0.39 ± 0.05
icf(N)	117.7 ± 19.7	4.07 ± 0.14	8.26 ± 0.77	3.04 ± 0.22	220.7 ± 17.0	9.05 ± 1.15	45.05 ± 9.80
$10^5 \times N/H$	1.29 ± 0.25	12.74 ± 0.53	61.45 ± 5.89	29.06 ± 2.27	4.19 ± 0.39	53.03 ± 7.85	17.57 ± 4.44
$10^5 \times O^+/H^+$	0.22 ± 0.028	10.51 ± 0.37	3.73 ± 0.12	18.79 ± 0.76	0.14 ± 0.01	1.68 ± 0.20	1.01 ± 0.21
$10^4 \times O^{++}/H^+$	2.32 ± 0.24	2.52 ± 0.07	1.52 ± 0.03	3.67 ± 0.14	2.36 ± 0.06	0.88 ± 0.03	4.08 ± 0.14
icf(O)	1.10 ± 0.04	1.20 ± 0.02	1.63 ± 0.14	1.03 ± 0.06	1.30 ± 0.01	1.45 ± 0.04	1.09 ± 0.06
$10^4 \times O/H$	2.59 ± 0.28	4.28 ± 0.12	3.08 ± 0.27	5.72 ± 0.35	3.09 ± 0.09	1.52 ± 0.07	4.55 ± 0.29
$10^5 \times Ne^{++}/H^+$	6.43 ± 0.44	8.21 ± 0.27	3.21 ± 0.07	19.93 ± 0.90	4.93 ± 0.14	2.65 ± 0.11	12.13 ± 0.50
$10^5 \times Ne^{3+}/H^+$			2.94 ± 0.10		0.53 ± 0.03	1.74 ± 0.10	0.48 ± 0.03
$10^5 \times Ne^{4+}/H^+$		0.19 ± 0.01	4.11 ± 0.08			2.04 ± 0.08	
icf(Ne)	1.12 ± 0.17	1.50	1.00	1.56 ± 0.07	1.31 ± 0.05	1.00	1.12 ± 0.08
$10^5 \times Ne/H$	7.20 ± 1.20	12.60 ± 0.27	10.26 ± 0.15	31.09 ± 1.98	6.46 ± 0.42	6.43 ± 0.17	13.58 ± 1.12
$10^8 \times Cl^{++}/H^+$		7.24 ± 0.18	3.14 ± 0.05	17.64 ± 0.60	2.00 ± 0.05	2.84 ± 0.09	7.60 ± 0.24
icf(Cl)		1.50 ± 0.10	1.81 ± 0.07	1.48 ± 0.09	4.26 ± 0.23	1.98 ± 0.14	2.59 ± 0.24
$10^7 \times Cl/H$		1.09 ± 0.07	0.57 ± 0.02	2.61 ± 0.19	0.85 ± 0.05	0.56 ± 0.04	1.97 ± 0.19
$10^7 \times S^+/H^+$		7.94 ± 0.16	3.61 ± 0.07	23.71 ± 0.58	0.093 ± 0.002	5.15 ± 0.35	1.52 ± 0.17
$10^6 \times S^{++}/H^+$	0.32 ± 0.40	3.26 ± 0.16	1.51 ± 0.03	7.69 ± 0.37	0.61 ± 0.02	1.60 ± 0.07	3.58 ± 0.15
icf(S)		1.21 ± 0.01	1.46 ± 0.04	1.13 ± 0.02	4.20 ± 0.11	1.50 ± 0.06	2.49 ± 0.18
$10^6 \times S/H$		4.89 ± 0.20	2.73 ± 0.09	11.37 ± 0.46	2.60 ± 0.11	3.17 ± 0.17	9.28 ± 0.75

and NGC 6302 as type I planetary nebulae (Peimbert 1978; Peimbert & Torres-Peimbert 1983), which represents objects rich in helium and nitrogen.

The S/O abundance ratios derived for our sample of planetary nebulae are 0.11 to 0.92 dex lower than the values estimated for H II regions and the Sun (Esteban et al. 1998; Grevesse et al. 1996), with considerably larger discrepancies for NGC 2438, NGC 2440 and NGC 3242. These subsolar S/O ratios for the planetary nebulae also found by other authors (Aller & Czyzak 1983; Aller & Keyes 1987; de Freitas Pacheco et al. 1991; Kingsburgh & Barlow 1994) were extensively discussed by Henry et al. (2004), who suggested that the problem lies in the S abundance estimates, which fail to adequately evaluate, through the use of icfs, the amount of S^{+3} in the planetary nebulae. In particular, the standard ionization corrections might not be adequate if a nebula is matter-bounded, as is often the case for planetary nebulae.

The O/H ratio for NGC 6302 is 0.2 to 0.5 dex lower than those obtained by other authors. Greater differences were found from Aller et al. (1981), who did not measure

Table 5. Comparison of elemental abundances from different sources.

Object	He	N	O	Ne	S	Cl	Ref.
NGC 1535	11.02	7.11	8.41	7.86			[1]
	10.96		8.58	7.97			[2]
	10.99	7.63	8.51	7.89			[3]
NGC 2438	11.05	8.10	8.63	8.11	6.69	5.04	[1]
	11.11	8.24	8.68				[5]
	11.15	8.00	8.38	7.60	6.51		[6]
NGC 2440	11.10	8.79	8.49	8.01	6.44	4.76	[1]
	11.18	9.09	8.82	8.14			[2]
	11.11	8.71	8.64	8.13	6.67		[6]
	11.08	8.98	8.64	7.95	6.30	5.11	[7]
	11.09	8.26	8.39	8.04			[8]
NGC 3132	11.10	8.46	8.77	8.49	7.06	5.42	[1]
	11.11	8.68	8.98	8.56			[2]
	11.08	8.37	8.82	8.49	7.02	5.36	[8]
NGC 3242	11.02	7.62	8.49	7.81	6.41	4.93	[1]
	11.03	7.71	8.72	8.03			[2]
	11.00	7.53	8.52	7.89	6.38	4.94	[8]
	10.96	7.96	8.64	8.04	6.51		[9]
	10.95	7.91	8.66	7.85	6.69	5.06	[4]
NGC 6302	11.18	8.72	8.18	7.81	6.50	4.75	[1]
	11.13	8.52	8.40	7.88	6.75	4.99	[8]
	11.23	8.76	8.41		6.69		[10]
	11.26	8.92	8.70	7.99	6.80	5.59	[11]
NGC 7009	11.07	8.24	8.66	8.13	6.97	5.29	[1]
	11.06	8.44	8.93	8.37			[2]
	11.07	8.40	8.66	8.04	6.98		[6]
	11.04	8.23	8.67	8.04	6.92		[12]
	11.07	8.10	8.68	8.16	7.12		[13]
Orion	10.99	7.78	8.72	7.89	7.17	5.33	[14]
Sun	10.99	7.97	8.87	8.08	7.33	5.50	[15]

References: [1] this paper; [2] Torres-Peimbert & Peimbert (1977); [3] Barker (1989); [4] Aller & Czyzak (1983); [5] Guerrero & Manchado (1999); [6] Kingsburgh & Barlow (1994); [7] Hyung & Aller (1998); [8] Tsamis et al. (2003); [9] Barker (1985); [10] de Freitas Pacheco et al. (1991); [11] Aller et al. (1981); [12] Gonçalves et al. (2003); [13] Barker (1983); [14] Esteban et al. (1998); [15] Grevesse et al. (1996).

the [O III]$\lambda\lambda$ 4959, 5007 lines. They calculated the chemical abundances with some measurements of emission line intensities combined with a simple theoretical model. For de Freitas Pacheco et al. (1991) and Tsamis et al. (2003), more modest differences of about 0.2 dex were found. In the case of the estimates of de Freitas Pacheco et al. (1991) the [O III]λ 4363 line was not measured; T_e(O III) was not adopted to calculate the O^{++}/H^+ abundance. The values of the oxygen emission line intensities, mean electron temperatures and densities adopted by Tsamis et al. (2003) to calculate the O^+/H^+ and O^{++}/H^+ and the ionic abundances are themselves very close to ours. However, they derived the O^{3+}/H^+ abundance from the O IV]λ 1401 ultraviolet line. Thus, their ionization correction scheme was simpler and the atomic abundance obtained is probably more precise than ours, since they only needed to indirectly evaluate the presence of oxygen ions with higher stages of ionization. The lack of O IV] line measurements should be less noticeable in low ionization objects. The central star of NGC 6302 is the hottest of our sample with a temperature of about 250 000 K (Casassus et al. 2000). This difference of about 0.2 dex in the O/H ratio gives a general idea of the errors in the total abundance for planetary nebulae with very hot central stars introduced by the use of different *icf*s.

Table 6. O^{++}/H^+ abundances derived from recombination lines.

		NGC 3242	NGC 7009
λ (Å)	Mult.	$O^{++}/H^+ \times 10^4$	$O^{++}/H^+ \times 10^3$
4662	1	5.91 ± 0.84	1.42 ± 0.07
4676	1		1.74 ± 0.10
4317	2		1.33 ± 0.04
4415	5	5.01 ± 1.25	2.51 ± 0.05
4132	19		0.90 ± 0.06
4155	19		1.99 ± 0.20
4089	48	5.27 ± 1.51	2.21 ± 0.08
4304	54		2.23 ± 0.15
4276	67	6.10 ± 2.71	1.92 ± 0.08
4284	67		1.84 ± 0.06
4609	92		2.62 ± 0.15
Average		5.57 ± 0.20	1.88 ± 0.14

Table 6 lists the O^{++}/H^+ abundance derived from recombination lines for NGC 3242 and NGC 7009. The values of the O^{++}/H^+ abundance estimated from different O II emission lines are quite similar to one another, both for NGC 3242 and NGC 7009. However, these abundances are significantly higher than those obtained from collisionally excited lines, by a factor of about two for NGC 3242 and of four for NGC 7009. Similar results were found by Liu et al. (1995) for NGC 7009 and by Tsamis et al. (2003, 2004) for NGC 3242.

Figure 2 presents the spatial profiles in the emission lines [O III]λ 4959, O II λ 4661, and Hβ for NGC 7009 along the East-West direction. The emission of [O III]λ 4959 and O II λ 4661 lines are more concentrated in the central region of the nebula, while the emission of Hβ line is distributed in a larger area of the nebula.

Figure 3 shows the spatial profiles for NGC 7009 of the O^{++}/H^+ abundances derived from recombination and forbidden lines and of the ratio between these two abundance estimates. The O^{++}/H^+ abundances derived from the O II λ 4661 recombination line are relatively constant

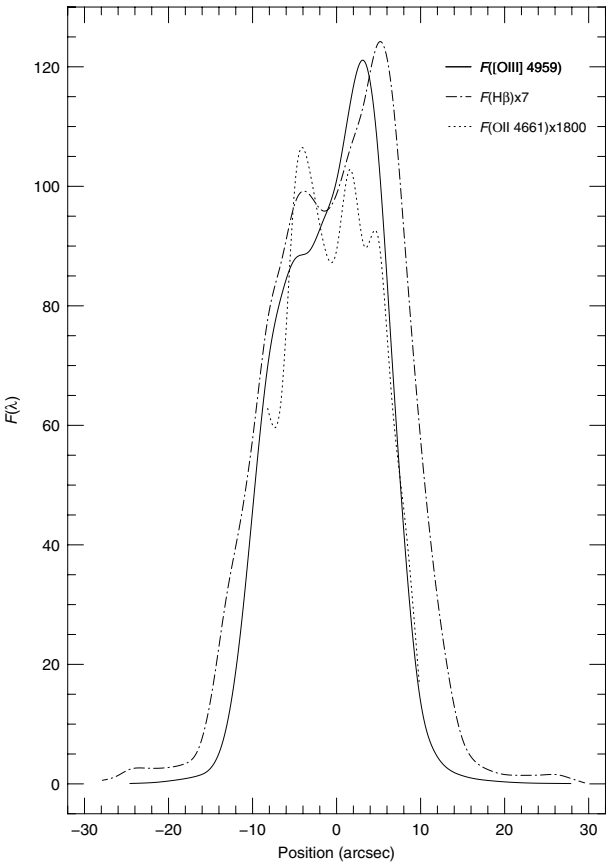

Fig. 2. Spatial profiles of the Hβ, [O III]λ 4959 and O IIλ 4661 fluxes (in units of 10^{-13} ergs cm^{-2} s^{-1}) for NGC 7009.

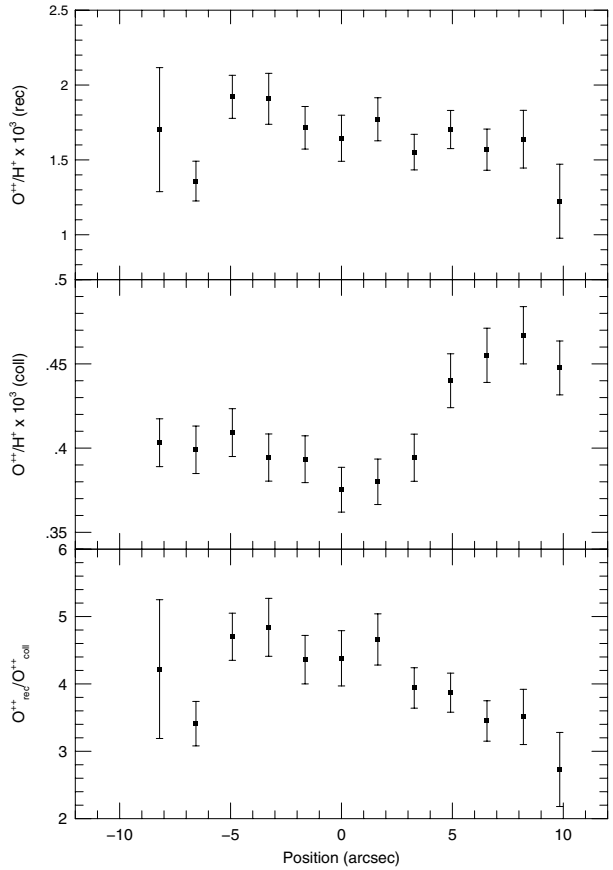

Fig. 3. Spatial profiles of the O^{++}/H^{+} abundances from the recombination line O IIλ 4661 (rec) and from the forbidden lines [O III]$\lambda\lambda$ 4959, 5007 (coll) and of the ratio between these two abundance estimates for NGC 7009.

along the nebular surface, while those derived from the [O III]$\lambda\lambda$ 4959, 5007 forbidden lines exhibit a strong variation across the nebula. Consequently, the ratio between the O^{++}/H^{+} abundances derived from recombination lines and those from forbidden lines is not constant along the nebular surface, decreasing smoothly from the center to the edges of the nebula (see Fig. 3, lower panel), which suggests that the discrepancy between abundances from permitted and forbidden lines is at least in part caused by a large scale spatial variation of some physical proprieties of the nebula and not entirely explained by localized fluctuations of any property. Interestingly, the discrepancy between O^{++}/H^{+} abundance from permitted and forbidden lines is also not constant along the nebular surface of the planetary nebulae NGC 6720 (Garnett & Dinerstein 2001) and NGC 6153 (Liu et al. 2000). For these nebulae, the differences in the O^{++}/H^{+} abundances are higher in the central part of the nebulae and lower in the outer regions of the nebulae.

We have looked for correlations between our O^{++} abundance ratios and some physical properties of NGC 7009 to explain these discrepancies. We found a relationship between the argon electron density estimate N_e(Ar IV) and O^{++} abundance ratio, with the abundance discrepancy increasing with the electron density (see Fig. 4).

One of the possible solutions to interpret the discrepancies between O^{++} abundances estimated from recombination lines and forbidden lines is the presence of electron temperature variations in ionized nebulae (Esteban et al. 1998, 1999; Peimbert et al. 1993; Ruiz et al. 2003; Peimbert et al. 2004). These temperature fluctuations were introduced by Peimbert (1967) and are usually characterized by the parameter t^2, the mean square temperature variation over the observed volume. If we assume that the ionic abundances derived from recombination lines are correct, we can estimate the t^2 value needed to obtain the same ionic abundances from forbidden lines, using the expressions given by Peimbert (1967) relating T_e(O III) to the t^2 and T_0. We can obtain compatible estimates of O^{++} derived from recombination and forbidden lines assuming a value of $t^2 \approx 0.09$ for both planetary nebulae NGC 3242 and NGC 7009.

Direct estimations of electron temperature fluctuations can be obtained through point-to-point measurements of the electron temperature across the nebula. In Paper I, we measured a temperature distribution with a variance relative to the mean corresponding to t_s^2(O III) = 0.0015 for NGC 3242 and t_s^2(O III) = 0.0023 for NGC 7009 from point-to-point measurements of [O III] electron temperature, which are much too low to have a significant impact on the determination of abundances derived from forbidden lines. However, as the temperature measured at any point is a mean value along the line of sight, t_s^2(O III) can only give a lower limit to t^2. From the difference between the [O III] and Balmer electron temperatures

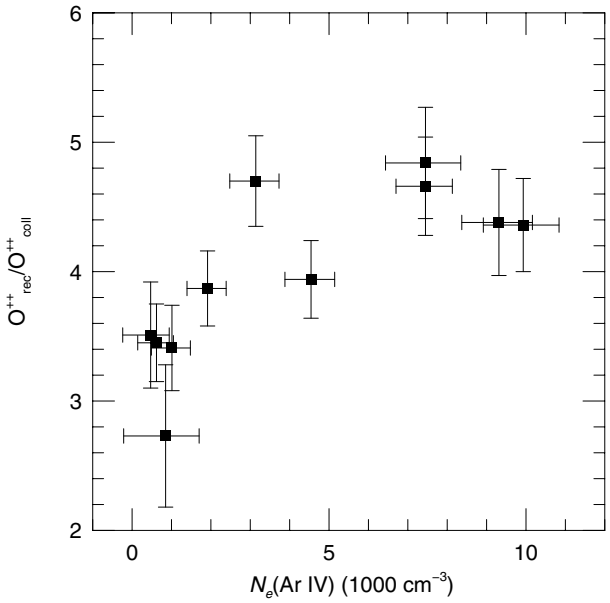

Fig. 4. Ratio between the values of O^{++}/H^+ derived from recombination and forbidden lines versus electron density N_e(Ar IV) for NGC 7009.

we have found $t^2 = 0.057$ for NGC 3242 and $t^2 = 0.027$ for NGC 7009, which are about two and three times lower than the value required to obtain the same abundances from recombination and forbidden lines, for NGC 3242 and NGC 7009, respectively. These differences between the [O III] and Balmer electron temperatures have been suggested as evidence in support of the presence of electron temperature fluctuations in gaseous nebulae to explain the discrepancies in abundances (Peimbert 1967; Liu & Danziger 1993).

Other explanation that has been suggested is the presence of abundance inhomogeneities in the nebulae (Torres-Peimbert et al. 1990; Peimbert 1993; Liu et al. 2000). Liu et al. (2000) have produced models for NGC 6153 that consider the presence of hydrogen deficient clumps, which occupy a small fraction of the volume of the nebula. In these models the heavy element recombination lines are produced in a dense and cool region, while the forbidden lines are emitted in a hotter and less dense region. These models seem to reproduce well the intensities of the recombination and collisionally excited lines. However, according to Ruiz et al. (2003) and Peimbert et al. (2004), the similarities found between the widths and radial velocities of the O II and [O III] lines in the planetary nebulae NGC 5307 and NGC 5315, imply that these lines are produced in the same regions, in contradiction to the hypothesis of chemical inhomogeneities. Also, the models of Liu et al. (2000) fail to reproduce the low Balmer temperature observed.

Unfortunately, we did not find sufficient evidence from our data to explain the abundance discrepancies detected in NGC 7009 and NGC 3242. Detailed observational studies about spatial variations of abundances from recombination and forbidden lines in more objects could provide clues to solve this problem.

4. Conclusions

A study on the determination of the elemental abundances from collisional excited and permitted lines in the galactic planetary nebulae NGC 1535, NGC 2438, NGC 2440, NGC 3132, NGC 3242, NGC 6302, and NGC 7009 is presented. The data analyzed were obtained with long-slit spectrophotometry of high signal-to-noise ratio in the range of 3100 to 6900 Å.

We found that the O^{++}/H^+ estimates derived from recombination lines are about a factor of four and two higher than those derived from forbidden lines for NGC 7009 and NGC 3242, respectively. The values of O^{++}/H^+ abundance estimated from different O II emission lines are similar to one another, both for NGC 3242 and NGC 7009. The differences between O^{++}/H^+ ratios derived from recombination lines and from forbidden lines decrease smoothly from the center to the edges in NGC 7009; this suggests that the discrepancies between the abundances from forbidden and permitted lines are at least in part caused by a large scale spatial variation of some physical proprieties of the nebula and not entirely explained by localized fluctuations of any single property. If we attribute these abundance differences to the presence of electron temperature fluctuations, a value of $t^2 \approx 0.09$ is required. However, direct estimations of electron temperature fluctuations were obtained through point-to-point measurements of the electron temperature across the nebula, with a variance relative to the mean corresponding to t^2_s(O III) = 0.0015 for NGC 3242 and t^2_s(O III) = 0.0023 for NGC 7009 (Paper I), which are much low to have a significant impact on the determination of abundances derived from forbidden lines.

Acknowledgements. This work was partially supported by the Brazilian institutions CAPES, CNPQ, and LNA.

References

Aller, L. H., & Czyzak, S. J. 1983, ApJS, 51, 211
Aller, L. H., & Keyes, C. D. 1987, ApJS, 65, 405
Aller, L. H., Ross, J. E., Omara, B. J., & Keyes, C. D. 1981, MNRAS, 197, 95
Barker, T. 1983, ApJ, 267, 630
Barker, T. 1985, ApJ, 294, 193
Barker, T. 1989, ApJ, 340, 921
Becker, S. R., Butler, K., & Zeippen, C. J. 1989, A&A, 221, 375
Benjamin, R. A., Skillman, E. D., & Smits, D. P. 1999, ApJ, 514, 307
Bhatia, A. K., & Kastner, S. O. 1988, ApJ, 332, 1063
Bhatia, A. K., & Doschek, G. A. 1993, ADNDT, 55, 315
Bowen, I. S. 1960, ApJ, 132, 1
Butler, K., & Zeippen, C. J. 1989, A&A, 208, 337
Butler, K., & Zeippen, C. J. 1994, A&AS, 108, 1
Casassus, S., Roche, P. F., & Barlow, M. J. 2000, MNRAS, 314, 657
de Freitas Pacheco, J. A., Maciel, W. J., Costa, R. D. D., & Barbuy, B. 1991, A&A, 250, 159
Esteban, C., Peimbert, M., Torres-Peimbert, S., & Escalante, V. 1998, MNRAS, 295, 401
Esteban, C., Peimbert, M., Torres-Peimbert, S., García-Rojas, J., & Rodríguez, M. 1999, ApJS, 120, 113
Fawcett, B. C. 1975, Atomic Data and Nuclear Data Tables, 16, 135
Galavis, M. E., Mendoza, C., & Zeippen, C. J. 1995, A&AS, 111, 347
Garnett, D. R., & Dinerstein, H. L. 2001, ApJ, 558, 145
Giles, K. 1981, MNRAS, 195, 63P

Gonçalves, D. R., Corradi, R. L. M., Mampaso, A., & Perinotto, M. 2003, ApJ, 597, 975
Grevesse, N., Noels, A., & Sauval, A. J. 1996, Cosmic Abundances, ASP Conf. Ser., 99, 117
Gruenwald, R., & Viegas, S. M. 1995, A&A, 303, 535
Guerrero, M. A., & Manchado, A. 1999, ApJ, 522, 378
Heise, C., Smith, P. L., & Calamai, A. G. 1995, ApJ, 451, L41
Henry, R. B. C., Kwitter, K. B., & Balick, B. 2004, AJ, 127, 2284
Hummer, D. G., & Storey, P. J. 1987, MNRAS, 224, 801
Hyung, S., & Aller, L. H. 1998, PASP, 110, 466
Kaufman, V., & Sugar, J. 1986, JPCRD, 15, 321
Keenan, F. P., Hibbert, A., Ojha, P. C., & Conlon, E. S. 1993, Phys. Scr. A., 48, 129
Kingdon, J. B., & Ferland, G. J. 1995, ApJ, 450, 691
Kingsburgh, R. L., & Barlow, M. J. 1994, MNRAS, 271, 257
Krabbe, A. C., & Copetti, M. V. F. 2002, A&A, 387, 295
Krabbe, A. C., & Copetti, M. V. F. 2005, A&A, 443, 981
LaJohn, L., & Luke, T., 1993, Phys. Scr. A., 47, 542
Lennon, D. J., & Burke, V. M. 1994, A&AS, 103, 273
Liu, X.-W. 1998, MNRAS, 295, 699
Liu, X.-W., & Danziger, I. J. 1993, MNRAS, 263, 256
Liu, X.-W., Storey, P. J., Barlow, M. J., & Clegg, R. E. S. 1995, MNRAS, 272, 369
Liu, X.-W., Storey, P. J., Danziger, I. J., Cohen, M., & Bryce, M. 2000, MNRAS, 312, 585
McLaughlin, B. M., & Bell, K. L. 1993, ApJ, 408, 753
Mendoza, C. 1983, Planetary Nebulae, IAU Symp., 103, 143
Mendoza, C., & Zeippen, C. J. 1982, MNRAS, 199, 1025
Moore, C. E. 1971, Selected Tables of Atomic Spectra, NSRDS-NBS, 35, 1
Moore, C. E. 1985, Selected Tables of Atomic Spectra, NSRDS-NBS 3, Sect. 11
O'Dell, C. R., Peimbert, M., & Peimbert, A. 2003, AJ, 125, 2590
Peimbert, M. 1967, ApJ, 150, 825
Peimbert, M. 1978, Planetary Nebulae, IAU Symp., 76, 215
Peimbert, M. 1993, Rev. Mex. Astron. Astrofis., 27, 9
Peimbert, M., & Torres-Peimbert, S. 1983, Planetary Nebulae, IAU Symp., 103, 233
Peimbert, M., Storey, P. J., & Torres-Peimbert, S. 1993, ApJ, 414, 626
Peimbert, M., Peimbert, A., Ruiz, M. T., & Esteban, C. 2004, ApJS, 150, 431
Pradhan, A. K. 1976, MNRAS, 177, 31
Ramsbottom, C. A., Bell, K. L., & Stafford, R. P. 1996, ADNDT, 63, 57
Rubin, R. H., Bhatt, N. J., Dufour, R. J., et al. 2002, MNRAS, 334, 777
Rubin, R. H., Martin, P. G., Dufour, R. J., et al. 2003, MNRAS, 340, 362
Ruiz, M. T., Peimbert, A., Peimbert, M., & Esteban, C. 2003, ApJ, 595, 247
Savage, B. D., & Mathis, J. S. 1979, ARA&A, 17, 73
Storey, P. J. 1994, A&A, 282, 999
Storey, P. J., & Hummer, D. G. 1995, MNRAS, 272, 41
Torres-Peimbert, S., & Peimbert, M. 1977, Rev. Mex. Astron. Astrofis., 2, 181
Torres-Peimbert, S., Peimbert, M., & Pena, M. 1990, A&A, 233, 540
Tsamis, Y. G., Barlow, M. J., Liu, X. -W., Danziger, I. J., & Storey, P. J. 2003, MNRAS, 345
Tsamis, Y. G., Barlow, M. J., Liu, X.-W., Storey, P. J., & Danziger, I. J. 2004, MNRAS, 353, 953
Verner D. A., Verner, E. M., & Ferland, G. J. 1996, ADNDT, 64, 1
Wiese, W. L., Fuhr, J. R., & Deters, T. M. 1996, JPCRD, Monograph 7
Williams, R. E., & Livio, M. 1995, Proc. of STScI 8, 24

Online Material

Table 1. Dereddened relative line fluxes $I(\lambda)$.

Line	$f(\lambda)$	NGC 1535 $I(\lambda)$	NGC 2438 $I(\lambda)$	NGC 2440 $I(\lambda)$	NGC 3132 $I(\lambda)$	NGC 3242 $I(\lambda)$	NGC 6302 $I(\lambda)$	NGC 7009 $I(\lambda)$
[Ne V] λ3346	0.389	...	...	97.21 ± 0.40	...	...	83.57 ± 0.43	...
O II + [Cl III]λ3354	0.386	...	...	...	...	...	...	0.38 ± 0.02
O III λ3405	0.364	...	...	...	0.22 ± 0.01	...	...	0.17 ± 0.02
O III + Ne II λ3415	0.360	...	...	...	0.18 ± 0.01	...	...	0.32 ± 0.02
[Ne V] λ3426	0.355	2.18 ± 0.08	5.93 ± 0.39	254.58 ± 0.70	...	1.73 ± 0.02	248.33 ± 1.00	...
O III λ3429	0.354		...		...			1.69 ± 0.03
O III λ3444	0.349	11.57 ± 0.12	...	20.10 ± 0.18	...	9.68 ± 0.02	18.14 ± 0.21	9.52 ± 0.04
He I λ3448	0.348	...	...		...	...	...	...
He I λ3468	0.342	...	...	...	...	...	0.82 ± 0.20	...
He I λ3479	0.339	...	...	...	...	...	...	0.12 ± 0.03
He I λ3488	0.336	...	...	...	...	...	...	0.08 ± 0.03
He I λ3499	0.334	...	...	...	...	0.05 ± 0.02	...	0.09 ± 0.03
He I λ3512	0.330	...	...	...	...	0.09 ± 0.02	...	0.16 ± 0.03
He I λ3530	0.325	...	...	...	...	0.14 ± 0.02	...	0.16 ± 0.03
He I λ3554	0.319	...	...	...	...	0.16 ± 0.02	0.55 ± 0.20	0.29 ± 0.03
Ne II λ3568	0.315	...	...	...	...	...	...	0.15 ± 0.03
He I λ3587	0.310	0.48 ± 0.07	...	...	...	0.17 ± 0.02	0.99 ± 0.21	0.32 ± 0.03
He I λ3614	0.303	...	...	...	...	0.09 ± 0.02	...	0.22 ± 0.03
He I λ3634	0.298	0.91 ± 0.07	...	...	...	0.27 ± 0.03	0.71 ± 0.22	0.48 ± 0.03
H I λ3687	0.284	0.55 ± 0.04	...	...	0.50 ± 0.12	0.18 ± 0.03	0.16 ± 0.22	0.15 ± 0.03
H I λ3692	0.283	0.60 ± 0.04	...	0.70 ± 0.14	0.54 ± 0.12	0.28 ± 0.03	0.26 ± 0.22	0.33 ± 0.03
H I λ3697	0.282	0.79 ± 0.04	...	1.11 ± 0.14	0.84 ± 0.13	0.43 ± 0.01	0.43 ± 0.22	0.53 ± 0.03
H I + He I λ3704	0.280	2.91 ± 0.05	...	2.00 ± 0.02	2.46 ± 0.26	1.46 ± 0.01	2.01 ± 0.22	1.82 ± 0.01
H I λ3712	0.278	2.55 ± 0.05	...	2.03 ± 0.02	1.76 ± 0.19	1.44 ± 0.01	1.33 ± 0.13	1.71 ± 0.01
[O II] λ3727	0.275	9.37 ± 0.08	441.56 ± 2.68	147.33 ± 0.32	532.75 ± 47.81	6.00 ± 0.02	115.68 ± 0.40	20.98 ± 0.04
H13 λ3734	0.273	2.90 ± 0.05	...	...	...	1.64 ± 0.01	...	1.94 ± 0.01
H12 λ3750	0.269	3.54 ± 0.05	4.83 ± 0.22	3.78 ± 0.03	3.73 ± 0.34	2.58 ± 0.01	2.27 ± 0.13	2.90 ± 0.01
O III λ3760	0.267	2.19 ± 0.05	...	5.34 ± 0.03	0.54 ± 0.11	3.77 ± 0.01	4.08 ± 0.13	2.20 ± 0.01
H11 λ3770	0.264	4.64 ± 0.06	5.76 ± 0.22	4.16 ± 0.03	5.23 ± 0.45	3.06 ± 0.01	3.24 ± 0.13	3.58 ± 0.01
H10 λ3798	0.258	6.06 ± 0.06	6.62 ± 0.23	5.85 ± 0.03	6.94 ± 0.58	3.86 ± 0.01	4.53 ± 0.13	4.83 ± 0.01
He II λ3813	0.254	...	...	0.39 ± 0.01	...	...	...	...
He I λ3820	0.253	1.41 ± 0.04	...	0.66 ± 0.02	2.31 ± 0.21	0.87 ± 0.01	1.24 ± 0.02	1.20 ± 0.01
H9 λ3835	0.249	8.67 ± 0.07	9.91 ± 0.23	9.20 ± 0.04	9.88 ± 0.78	6.11 ± 0.02	6.97 ± 0.04	7.31 ± 0.01
[Ne III] λ3869	0.242	115.84 ± 0.22	115.33 ± 1.02	106.46 ± 0.21	145.33 ± 10.94	88.84 ± 0.06	158.66 ± 0.46	109.75 ± 0.12
He I + H8 λ3889	0.237	24.72 ± 0.10	22.91 ± 0.34	18.00 ± 0.06	29.99 ± 2.21	16.30 ± 0.02	21.58 ± 0.07	19.70 ± 0.02
He II λ3923	0.230	...	...	0.66 ± 0.01	...	0.37 ± 0.02	0.63 ± 0.02	...
[Ne III] λ3967	0.220	55.75 ± 0.13	28.27 ± 0.31	31.89 ± 0.12	55.66 ± 3.71	22.74 ± 0.10	62.90 ± 0.18	49.82 ± 0.04
H7 λ3970	0.220		12.79 ± 0.22	12.34 ± 0.07		19.82 ± 0.09		
He I λ4009	0.211	0.25 ± 0.02	...	...	...	0.21 ± 0.02	...	0.19 ± 0.01
He I λ4026	0.207	2.53 ± 0.03	2.75 ± 0.20	2.25 ± 0.05	3.07 ± 0.20	2.11 ± 0.05	3.38 ± 0.04	2.49 ± 0.01
[S II] + O II λ4069	0.198	1.08 ± 0.03	4.00 ± 0.20	3.27 ± 0.05	6.95 ± 0.41	1.16 ± 0.04	11.66 ± 0.05	1.86 ± 0.02
[S II] + O II λ4076	0.196		1.34 ± 0.07	0.89 ± 0.04	2.60 ± 0.16	0.35 ± 0.02	3.85 ± 0.04	0.88 ± 0.02
O II λ4084	0.195	...	...	...	...	0.05 ± 0.02	...	...
O II λ4089	0.194	...	...	...	...	0.07 ± 0.02	...	0.28 ± 0.01
N III + O II λ4097	0.192	...	...	3.01 ± 0.03	...	1.74 ± 0.05	...	...
Hδ λ4101	0.191	29.92 ± 0.08	27.88 ± 0.28	29.30 ± 0.05	26.14 ± 1.48	27.04 ± 0.07	25.90 ± 0.08	25.93 ± 0.07
O II + He I λ4120	0.187	0.26 ± 0.02	...	0.40 ± 0.02	0.54 ± 0.06	0.37 ± 0.02	0.61 ± 0.04	0.45 ± 0.01
O II λ4129	0.185	...	...	...	...	0.10 ± 0.02	...	...
O II λ4133	0.184	...	...	...	...	...	...	0.05 ± 0.003
He I λ4144	0.182	0.36 ± 0.02	...	0.34 ± 0.02	0.58 ± 0.06	0.31 ± 0.02	0.48 ± 0.04	0.40 ± 0.01
O II λ4155	0.180	...	...	...	...	...	...	0.14 ± 0.01
[K V] λ4163	0.178	...	...	0.24 ± 0.02	...	...	0.38 ± 0.04	...
He I + O II λ4169	0.177	...	...	...	0.19 ± 0.04	...	0.13 ± 0.04	0.08 ± 0.01
N II λ4176	0.175	...	...	...	...	...	...	0.02 ± 0.003
N II λ4180	0.174	...	...	0.05 ± 0.01	...	...	...	0.03 ± 0.003
O II + C III λ4186	0.173	...	...	0.28 ± 0.01	...	0.33 ± 0.02	...	0.20 ± 0.003
He II λ4200	0.170	0.41 ± 0.02	...	1.64 ± 0.03	0.20 ± 0.04	0.68 ± 0.04	1.46 ± 0.05	0.34 ± 0.01
Ne II λ4220	0.166	...	...	...	...	...	...	0.08 ± 0.003

Table 1. continued.

Line	$f(\lambda)$	NGC 1535 $I(\lambda)$	NGC 2438 $I(\lambda)$	NGC 2440 $I(\lambda)$	NGC 3132 $I(\lambda)$	NGC 3242 $I(\lambda)$	NGC 6302 $I(\lambda)$	NGC 7009 $I(\lambda)$
N II+ Fe V λ4228	0.165	0.37 ± 0.02	...	0.56 ± 0.02	...	0.15 ± 0.01	0.41 ± 0.05	0.25 ± 0.01
N II λ4237	0.163	...	...	...	...	...	...	0.10 ± 0.003
N II λ4242	0.162	...	...	...	...	...	...	0.05 ± 0.003
O II λ4254	0.160	...	...	...	...	...	...	0.05 ± 0.003
C II λ4267	0.157	0.36 ± 0.02	1.26 ± 0.07	0.43 ± 0.02	0.82 ± 0.06	0.77 ± 0.04	0.16 ± 0.05	0.87 ± 0.01
O II λ4276	0.155	...	...	...	...	0.09 ± 0.04	...	0.27 ± 0.01
O II λ4284	0.154	...	...	...	...	...	...	0.10 ± 0.003
O II λ4304	0.150	...	...	...	...	...	...	0.13 ± 0.01
O II λ4317	0.147	...	...	...	...	...	...	0.23 ± 0.01
Hγ λ4340	0.143	46.80 ± 0.08	46.80 ± 0.29	46.80 ± 0.12	46.80 ± 1.98	46.80 ± 0.08	46.80 ± 0.13	46.80 ± 0.08
[O III] λ4363	0.138	12.65 ± 0.04	9.56 ± 0.15	23.98 ± 0.07	4.56 ± 0.19	14.05 ± 0.04	36.46 ± 0.10	7.57 ± 0.02
Ne II + N III λ4379	0.135	0.16 ± 0.01	...	0.44 ± 0.02	...	0.23 ± 0.01	0.17 ± 0.05	0.45 ± 0.01
He II λ4388	0.134	0.58 ± 0.01	...	0.32 ± 0.01	0.75 ± 0.04	0.40 ± 0.01	0.62 ± 0.05	0.57 ± 0.01
Ne II λ4409	0.129	...	...	...	...	...	...	0.04 ± 0.004
O II λ4415	0.127	...	...	...	...	0.04 ± 0.01	...	0.20 ± 0.004
He I λ4471	0.110	4.06 ± 0.02	4.46 ± 0.13	2.86 ± 0.02	5.74 ± 0.20	3.52 ± 0.03	5.90 ± 0.05	5.00 ± 0.02
C II + O II λ4491	0.104	...	...	...	...	...	...	0.09 ± 0.004
N III λ4511	0.098	...	...	0.34 ± 0.01	...	0.11 ± 0.03	...	0.17 ± 0.01
N III λ4518	0.096	...	...	...	...	...	...	0.14 ± 0.01
N III λ4524	0.094	...	...	...	...	...	...	0.05 ± 0.01
N II + N III λ4530	0.092	...	...	...	...	...	...	0.06 ± 0.01
N III λ4535	0.091	...	...	...	...	...	...	0.07 ± 0.01
He II λ4541	0.089	0.66 ± 0.01	1.67 ± 0.07	2.75 ± 0.02	0.37 ± 0.02	1.22 ± 0.03	2.53 ± 0.02	0.55 ± 0.01
N II λ4552	0.085	...	...	...	...	...	...	0.24 ± 0.01
Mg I] λ4562	0.083	...	1.00 ± 0.06	0.14 ± 0.01	0.38 ± 0.02	...	...	0.07 ± 0.01
Mg I] λ4571	0.080	...	0.60 ± 0.05	0.21 ± 0.01	0.36 ± 0.02	...	0.22 ± 0.01	0.09 ± 0.01
O II λ4591	0.074	...	...	...	...	...	...	0.08 ± 0.01
O II λ4596	0.073	...	...	...	...	...	...	0.05 ± 0.01
N II λ4601	0.071	...	...	...	...	...	...	0.04 ± 0.01
N V + O II λ4604	0.070	...	...	0.10 ± 0.01	...	...	...	...
[Fe III] + N II λ4606	0.070	...	...	0.47 ± 0.01	...	...	0.57 ± 0.01	...
O II λ4609	0.069	...	...	...	...	...	...	0.16 ± 0.01
N III λ4634	0.062	0.43 ± 0.01	...	1.89 ± 0.02	0.21 ± 0.02	1.01 ± 0.03	2.63 ± 0.02	1.19 ± 0.01
N III + O II λ4641	0.060	1.08 ± 0.01	...	4.12 ± 0.02	0.83 ± 0.03	2.60 ± 0.03	5.68 ± 0.06	3.28 ± 0.02
C III λ4647	0.058	0.65 ± 0.01	...	0.18 ± 0.01	...	0.22 ± 0.04	...	0.97 ± 0.01
O II + C III λ4650	0.057		...	0.32 ± 0.01	0.36 ± 0.02	0.70 ± 0.02	...	
[Fe III] + C IV λ4658	0.055	...	...	1.02 ± 0.02	...	0.20 ± 0.01	0.50 ± 0.01	0.12 ± 0.01
O II λ4662	0.054	...	...	...	...	0.07 ± 0.01	...	0.18 ± 0.01
O II λ4676	0.050	...	...	...	...	...	...	0.17 ± 0.01
He II λ4686	0.047	16.98 ± 0.04	31.72 ± 0.16	74.86 ± 0.11	7.07 ± 0.21	40.53 ± 0.05	71.40 ± 0.54	17.06 ± 0.06
[Ar IV] + He I λ4712	0.040	4.53 ± 0.02	1.91 ± 0.07	11.08 ± 0.04	1.29 ± 0.04	5.95 ± 0.02	14.97 ± 0.04	4.54 ± 0.02
[Ne IV] λ4725	0.036	...	...	1.79 ± 0.02	...	0.12 ± 0.01	3.23 ± 0.03	0.04 ± 0.01
[Ar IV] λ4740	0.032	3.36 ± 0.02	1.25 ± 0.06	9.32 ± 0.03	0.62 ± 0.02	5.29 ± 0.02	18.31 ± 0.07	4.39 ± 0.02
C II + N II λ4802	0.016	...	...	0.09 ± 0.01	...	...	...	...
Hβ λ4861	0.000	100.00 ± 0.10	100.00 ± 0.30	100.00 ± 0.13	100.00 ± 2.95	100.00 ± 0.10	100.00 ± 0.18	100.00 ± 0.19
[Fe III] λ4881	-0.005	...	...	0.19 ± 0.02	...	...	...	...
He I λ4922	-0.016	1.11 ± 0.01	0.84 ± 0.09	0.73 ± 0.02	1.44 ± 0.04	0.90 ± 0.02	1.43 ± 0.03	1.49 ± 0.02
[O III] λ4932	-0.018	0.13 ± 0.01	...	0.30 ± 0.02	...	0.26 ± 0.02	0.28 ± 0.03	0.13 ± 0.01
O II λ4943	-0.021	...	...	...	...	...	0.46 ± 0.03	...
N V λ4945	-0.021	...	...	0.22 ± 0.02	...	...	...	...
[O III] λ4959	-0.025	405.88 ± 0.94	358.18 ± 0.90	450.38 ± 0.10	287.46 ± 1.06	416.43 ± 0.36	424.98 ± 2.81	390.25 ± 0.59
[O III] λ5007	-0.037	1189.38 ± 2.56	1045.42 ± 2.57	1312.31 ± 3.01	885.72 ± 3.17	1204.84 ± 1.02	1271.16 ± 9.04	1170.75 ± 1.77
He I λ5015	-0.039	...	0.92 ± 0.10	...	...	...	...	...
[N I] λ5200	-0.082	...	...	8.71 ± 0.07	9.73 ± 0.15	...	19.49 ± 0.39	...
He II λ5412	-0.128	1.27 ± 0.04	3.19 ± 0.24	7.03 ± 0.07	...	3.02 ± 0.02	5.02 ± 0.31	1.24 ± 0.01
[Cl III] λ5517	-0.149	...	0.98 ± 0.24	0.55 ± 0.06	1.23 ± 0.07	0.26 ± 0.02	0.54 ± 0.06	0.48 ± 0.01
[Cl III] λ5537	-0.153	...	0.54 ± 0.24	0.66 ± 0.06	1.06 ± 0.07	0.25 ± 0.02	0.88 ± 0.06	0.59 ± 0.01
N II λ5667	-0.176	...	...	...	...	...	...	0.05 ± 0.01

Table 1. continued.

		NGC 1535	NGC 2438	NGC 2440	NGC 3132	NGC 3242	NGC 6302	NGC 7009
Line	$f(\lambda)$	$I(\lambda)$	$I(\lambda)$	$I(\lambda)$	$I(\lambda)$	$I(\lambda)$	$I(\lambda)$	$I(\lambda)$
N II λ5669	−0.176	...	...	...	...	...	...	0.16 ± 0.01
[N II] λ5755	−0.191	...	3.79 ± 0.25	11.70 ± 0.09	8.22 ± 0.10	...	19.80 ± 0.46	0.46 ± 0.01
C IV λ5802	−0.198	...	...	...	...	0.35 ± 0.02	...	...
C IV λ5812	−0.200	...	...	...	...	0.20 ± 0.02	...	...
He I λ5876	−0.210	12.63 ± 0.04	11.56 ± 0.34	8.24 ± 0.08	17.25 ± 0.17	10.26 ± 0.03	19.08 ± 0.48	15.70 ± 0.04
He II λ6037	−0.235	...	...	...	...	...	...	0.45 ± 0.03
K IV λ6102	−0.245	...	...	...	...	0.28 ± 0.03	...	...
He II λ6171	−0.255	...	...	...	...	0.14 ± 0.03	...	...
He II λ6234	−0.264	...	...	0.32 ± 0.04	...	0.13 ± 0.03	...	...
[O I] λ6300	−0.274	0.10 ± 0.03	31.77 ± 0.88	14.26 ± 0.11	33.55 ± 0.37	0.12 ± 0.03	24.39 ± 0.75	0.71 ± 0.03
[S III] λ6312	−0.275	0.28 ± 0.03	2.18 ± 0.20	2.51 ± 0.04	2.58 ± 0.06	0.53 ± 0.03	5.09 ± 0.20	1.54 ± 0.03
[O I] λ6364	−0.282	0.24 ± 0.03	9.86 ± 0.34	4.87 ± 0.05	11.61 ± 0.14	0.13 ± 0.03	7.95 ± 0.28	...
[S III] λ6312	−0.275	0.28 ± 0.03	2.18 ± 0.20	2.51 ± 0.04	2.58 ± 0.06	0.53 ± 0.03	5.09 ± 0.20	1.54 ± 0.03
[O I] λ6364	−0.282	0.24 ± 0.03	9.86 ± 0.34	4.87 ± 0.05	11.61 ± 0.14	0.13 ± 0.03	7.95 ± 0.28	...
He II λ6406	−0.288	...	...	0.32 ± 0.03	...	0.17 ± 0.03	...	...
[Ar V] λ6435	−0.292	...	...	2.58 ± 0.04	...	0.12 ± 0.03	4.52 ± 0.19	...
C II λ6462	−0.296	...	...	...	...	0.12 ± 0.01	...	...
He II + [N II] λ6527	−0.304	...	...	0.62 ± 0.03	...	0.17 ± 0.01	...	...
[N II] λ6548	−0.307	...	71.40 ± 2.14	186.43 ± 1.49	179.69 ± 2.15	0.50 ± 0.01	209.84 ± 7.14	7.23 ± 0.04
Hα λ6562	−0.308	...	286.00 ± 8.58	286.00 ± 2.28	286.00 ± 3.44	...	286.00 ± 9.78	286.00 ± 0.98
[N II] λ6583	−0.311	0.85 ± 0.01	212.67 ± 6.44	566.03 ± 4.55	...	1.51 ± 0.02	646.88 ± 22.31	21.94 ± 0.08
He II λ6678	−0.323	3.36 ± 0.01	3.36 ± 0.25	3.04 ± 0.04	4.03 ± 0.08	2.59 ± 0.02	3.21 ± 0.18	3.53 ± 0.04
[S II] λ6717	−0.328	...	24.90 ± 0.82	7.484 ± 0.07	50.81 ± 0.66	0.24 ± 0.01	13.85 ± 0.52	1.74 ± 0.04
[S II] λ6731	−0.330	...	19.40 ± 0.66	9.75 ± 0.09	51.42 ± 0.67	0.26 ± 0.01	19.04 ± 0.71	2.83 ± 0.04
c(Hβ)		0.01	0.20	0.40	0.17	0.10	0.90	0.22